Structural Chemistry (2023) 34:639–653
https://doi.org/10.1007/s11224-022-02006-x

ORIGINAL RESEARCH

Synthesis and DFT analysis of non-covalent interactions in crystal structures of 6-R-2-alkoxy-, 2,3-di-, and 2,2,3-tri-*tert*-butylpyrrolo[1,2-*b*][1,2,4]triazines

Denis S. Koltun[1] · **Sergey M. Ivanov**[1]

Received: 20 May 2022 / Accepted: 28 June 2022 / Published online: 20 July 2022

Abstract
Novel 7-amino-3-*tert*-butyl-2-OR[1]-6-R[2]-pyrrolo[1,2-*b*][1,2,4]triazine-8-carbonitriles ($R^1 = CH_2CO_2Et$, CH_2Boc, Me, *n*-Bu; $R^2 = CO_2Et$, CO_2*n*-Bu, CO_2*t*-Bu, $C_6H_4CO_2$*i*-Pr) have been synthesized and investigated by X-ray diffraction. Nucleophilic replacement of an alkoxy group with *t*-BuLi afforded sterically hindered *tert*-butyl 7-amino-2,3-di-*tert*-butyl- and 2,2,3-tri-*tert*-butyl-8-cyanopyrrolo[1,2-*b*][1,2,4]triazine-6-carboxylates. The lengths and bond angles as well as packing modes of molecules in crystals have been considered. The non-covalent interactions such as the changes in the H-bonding and close contacts were analyzed by DFT and the Hirshfeld surfaces and compared for different substituents.

Keywords Crystal structure · X-ray diffraction · 1,2,4-triazine · pyrrolo[1,2-*b*][1,2,4]triazine · DFT calculation · Hirshfeld surface analysis

Introduction

Six-membered heterocycles containing one or two nitrogen atoms are ubiquitous in plants as alkaloids with a broad range of biological activities [1, 2]. Triazines are rarely found in nature (e.g., fervenulin, toxoflavin [3, 4], and fluviols [5]); nevertheless, they also exhibit antibacterial, antifungal, and anticancer properties [6], which make them an important target for research and various applications. Azolotriazines are particularly interesting in terms of their diverse chemical transformations and the bioisosteric nature [7]. The quantitative and qualitative structural analysis of known azolo[1,2,4]triazines, along with molecular modeling, has been successfully used to identify the most privileged scaffolds for further drug design [8–10]. These developments resulted in the production of the 4-aminopyrrolo[2,1-*f*][1,2,4]triazine remdesivir, which is active against a number of viruses including Ebola virus and coronaviruses [11]. The interactions between an inhibitor and its molecular target are considered primarily non-covalent in nature and shape dependent. Therefore, the changes in the H-bonding and hydrophobic nature of the substituents can greatly affect the biological potency of the compounds [12–14]. It seems clear that investigation of such structural relationships, including novel hydrophilic and hydrophobic cases, can further shed the light on mechanism of influence of different substituent configurations on the binding affinity.

Recently, we have investigated 2-alkoxy- and alkylthiopyrrolo[1,2,4]triazines with a moderate antimicrobial activity [15] synthesized by recyclization of pyrazolo[5,1-*c*][1,2,4]triazines and (1,2,4-triazin-3(2*H*)-ylidene)acetonitriles [16, 17]. In continuation of our studies, in the present work, we discuss the X-ray structures of novel 7-amino-3-*tert*-butyl-2-alkoxy-, 2,3-di-*tert*-butyl-, and 2,2,3-tri-*tert*-butylpyrrolo[1,2-*b*][1,2,4]triazine-8-carbonitriles, as well as the non-covalent interactions and packing modes in the single crystals.

Experimental

General experimental remarks

Melting points were determined on a STUART Melting point SMP30 apparatus. IR spectra were recorded in KBr

✉ Denis S. Koltun
deniscoltun@yandex.ru

[1] N.D. Zelinsky Institute of Organic Chemistry, Russian Academy of Sciences, 47 Leninsky Prospect, Moscow, Russian Federation, Russia 119991

pellets using Agilent Cary 660 FTIR infrared spectrophotometer. NMR spectra were recorded on Bruker AM-300, DRX-500, or AV-600 spectrometers operating at working frequencies of 300, 600 (^{1}H), 75, 126, or 151 MHz (^{13}C). Chemical shifts were related to that of the $CHCl_3$ (^{1}H), or $CDCl_3$ (^{13}C). High-resolution mass spectra were recorded on a Bruker MicroTOF II instrument in positive ion mode (capillary voltage 4500 V) using electrospray ionization (ESI) and methanol or acetonitrile as a solvent. Elemental analysis was performed on a PerkinElmer Series II 2400 Elemental Analyzer. All reagents were obtained from commercial sources and used without additional purification. All operations, except for chromatography, were carried out in argon atmosphere. Starting compound **1** was synthesized as described in literature [18].

General procedure for the synthesis of compounds 2a,b and 3 (Scheme 1)

Compound **1** (0.35 g, 1.61 mmol) was dissolved in 20 ml of dry DMF. To the resulting solution, powdered KOH (0.5 g, 8.91 mmol) was added in one portion. After stirring at r.t. for 15 min, the corresponding alkyl bromoacetate (5 mmol, for the synthesis of **2a,b**) or isopropyl (*p*-bromomethyl)benzoate (2 mmol of $BrCH_2C_6H_4CO_2i$-Pr for **3**) was added, and the reaction mixture was stirred at r.t. for 24 h (for the synthesis of **2a,b**) or at 50 °C for 3 h (for the synthesis of **3**). Next, an additional portion of alkyl bromoacetate (5 mmol) was added, and the stirring was continued at r.t. for 24 h. The reaction mixture was decanted and quenched with cooled H_2O (200 ml) with vigorous stirring, followed by extraction with dichloromethane (3 × 50 ml). The combined organic phases were washed with H_2O (3 × 100 ml), dried with crystalline K_2CO_3, and filtered. The solvents were removed in vacuo, and the residue was purified by flash column chromatography (eluted with EtOAc:heptane = 1:10–1:3) to give compounds **2a,b** and **3**. Spectral data for compound **2b**, bright yellow powder, yield 0.63 g (1.41 mmol, 88%), mp. 185–186 °C, coincided with those described in literature [15].

Ethyl 7-amino-3-*tert*-butyl-8-cyano-2-(2-ethoxy-2-oxoethoxy) pyrrolo[1,2-*b*][1,2,4]triazine-6-carboxylate (2a) Bright yellow crystals, yield 0.51 g (1.31 mmol, 81%), mp. 160–162 °C (decomp.). IR (KBr) ν = 3419, 3332, 3273, 3228, 3213 (NH), 2979, 2939, 2909, 2873 (CH), 2218 (CN), 1748, 1661, 1623 (2 C=O), 1597, 1552, 1522, 1489, 1447, 1405, 1368, 1346, 1314, 1257, 1197, 1158, 1132, 1114, 1053, 1028, 947, 927, 878, 856, 766, 757, 731, 680, 664, 622, 540, 512, 477, 429 cm^{-1}. ^{1}H NMR: (300 MHz, $CDCl_3$) δ 1.33 (t, J = 7.2 Hz, 3H, C(6)–$CO_2CH_2C\underline{H}_3$), 1.41 (t, J = 7.1 Hz, 3H, $CH_2CO_2CH_2C\underline{H}_3$), 1.49 (s, 9H, Bu^t), 4.29 (q, J = 7.1 Hz, 2H, C(6)–$CO_2C\underline{H}_2CH_3$), 4.39 (q, J = 7.0 Hz, 2H, $CH_2CO_2C\underline{H}_2CH_3$), 5.10 (s, 2H, $C\underline{H}_2CO_2Et$), 5.61 (br. s, 2H, $N\underline{H}_2$). ^{13}C{^{1}H} NMR: (APT, 75 MHz, $CDCl_3$) δ 14.15, 14.47 (2 $CO_2CH_2C\underline{H}_3$), 27.83 ($C(\underline{C}H_3)_3$), 37.44 ($\underline{C}(CH_3)_3$), 60.05, 61.77, 63.04 (C(6)–$CO_2\underline{C}H_2CH_3$, $\underline{C}H_2C$-$O_2\underline{C}H_2CH_3$), 113.17 ($\underline{C}N$), 69.50, 100.16, 138.55, 147.95, 148.21, 153.50 (C(2), C(3), C(6), C(7), C(8), C(8a)), 161.09, 167.10 (2 $\underline{C}O_2Et$). HRMS m/z ($I_{rel.}$ %) calculated: 390.1772 $[M+H]^+$, found: 390.1764 $[M+H]^+$ (100). Anal. calcd. for $C_{18}H_{23}N_5O_5$ (%): C, 55.52, H, 5.95, N, 17.98. Found (%): C, 55.48, H, 5.91, N, 17.96.

Isopropyl 4-(7-amino-2-(2-*tert*-butoxy-2-oxoethoxy)-3-*tert*-butyl-8-cyanopyrrolo[1,2-*b*][1,2,4]triazin-6-yl)benzoate (3) Orange crystals, yield 0.60 g (1.18 mmol, 73%), mp. 181–184 °C. IR (KBr) ν = 3441, 3364, 3249 (NH), 2978,

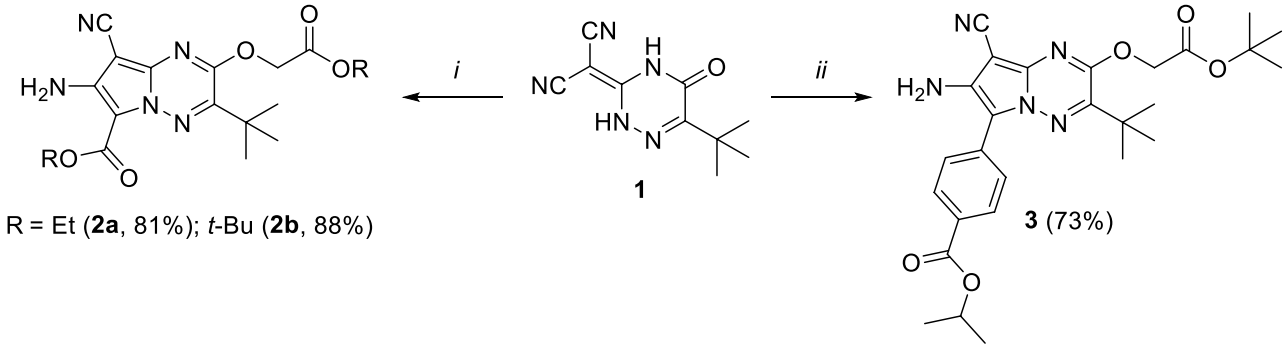

R = Et (**2a**, 81%); *t*-Bu (**2b**, 88%)

Reagents and conditions:

i: $BrCH_2CO_2Et$ (R=Et) or $BrCH_2CO_2t$-Bu (R=*t*-Bu), KOH, DMF, 20°C, 48 h;

ii: $BrCH_2C_6H_4CO_2i$-Pr, KOH, DMF, 50°C, 3 h, then $BrCH_2CO_2t$-Bu, 20°C, 24 h.

Scheme 1 Synthesis of compounds 2a,b and 3

2937, 2873 (CH), 2220 (CN), 1758, 1704, 1648 (2 C = O), 1606, 1564, 1548, 1533, 1514, 1478, 1432, 1397, 1368, 1353, 1314, 1279, 1225, 1182, 1150, 1127, 1101, 1076, 1053, 1022, 918, 889, 865, 851, 835, 775, 761, 747, 700, 673, 634, 569, 586, 502, 473, 426, 443 cm^{-1}. ^1H NMR: (300 MHz, $CDCl_3$) δ 1.40 (d, $J = 5.9$ Hz, 6H, $(CH_3)_2CH–O$), 1.46, 1.53 (2 s, 9 + 9 H, 2 Bu^t), 4.24 (s, 2H, NH_2), 4.95 (s, 2H, $CH_2CO_2Bu^t$), 5.28 (p, $J = 6.3$ Hz, 1H, $(CH_3)_2CH–O$), 7.81 (d, $J = 8.1$ Hz, 2H, 2 *o*–CH Ar), 8.13 (d, $J = 8.2$ Hz, 2H, 2 m-CH Ar). $^{13}C\{^1H\}$ NMR: (APT, 126 MHz, $CDCl_3$) δ 21.98 ($(CH_3)_2CH–O$), 27.93, 28.08 (2 $C(CH_3)_3$), 37.38 (C(3)–$C(CH_3)_3$), 63.57 ($CH_2CO_2Bu^t$), 68.41 ($(CH_3)_2CH–O$), 82.88 (O–$C(CH_3)_3$), 114.00 (CN), 126.62, 129.93 (2 *o*–CH and 2 m-CH Ar), 70.68, 108.11, 128.63, 133.35, 135.56, 137.59, 147.72, 151.98 (C(2), C(3), C(6), C(7), C(8), C(8a) and 2 *ipso*-C Ar), 165.70, 166.48 (CO_2Bu^t and CO_2Pr^i). HRMS *m/z* ($I_{rel.}$ %) calculated: 508.2554 $[M + H]^+$, found: 508.2550 $[M + H]^+$ (100). Anal. calcd. for $C_{27}H_{33}N_5O_5$ (%): C, 63.89, H, 6.55, N, 13.80. Found (%): C, 63.94, H, 6.52, N, 13.81.

General procedure for the synthesis of compounds 2c–e (Scheme 2)

Compound **2a** or **2b** (0.51 mmol) was dissolved in 10 ml of dry MeOH (for the synthesis of **2d**), 5 ml of dry ethylene glycol (for **2e**), or 5 ml of *n*-butanol (for **2c,f**). Next, powdered K_2CO_3 (0.1 g, 0.72 mmol) was added in one portion, and the reaction mixture was heated under reflux for 40 min (for **2d**), 5 h (for **2c,f**), or at 100 °C for 1 h (for **2e**). After cooling to r.t., EtOAc (30 ml) was added with stirring. The resulting mixture was filtered, the solvents were removed in vacuo, and the residue was purified by flash column chromatography (eluted with EtOAc:heptane = 1:30–1:5) to give compounds **2c–f**. Spectral and X-ray data for compound **2c**, pale yellow crystals (CCDC 2,017,998), yield 0.17 g (0.44 mmol, 86%), mp. 159–160 °C, coincided with those described in literature [16].

Ethyl 7-amino-3-*tert*-butyl-8-cyano-2-methoxypyrrolo[1,2-*b*][1,2,4]triazine-6-carboxylate (2d) Colorless crystals, yield

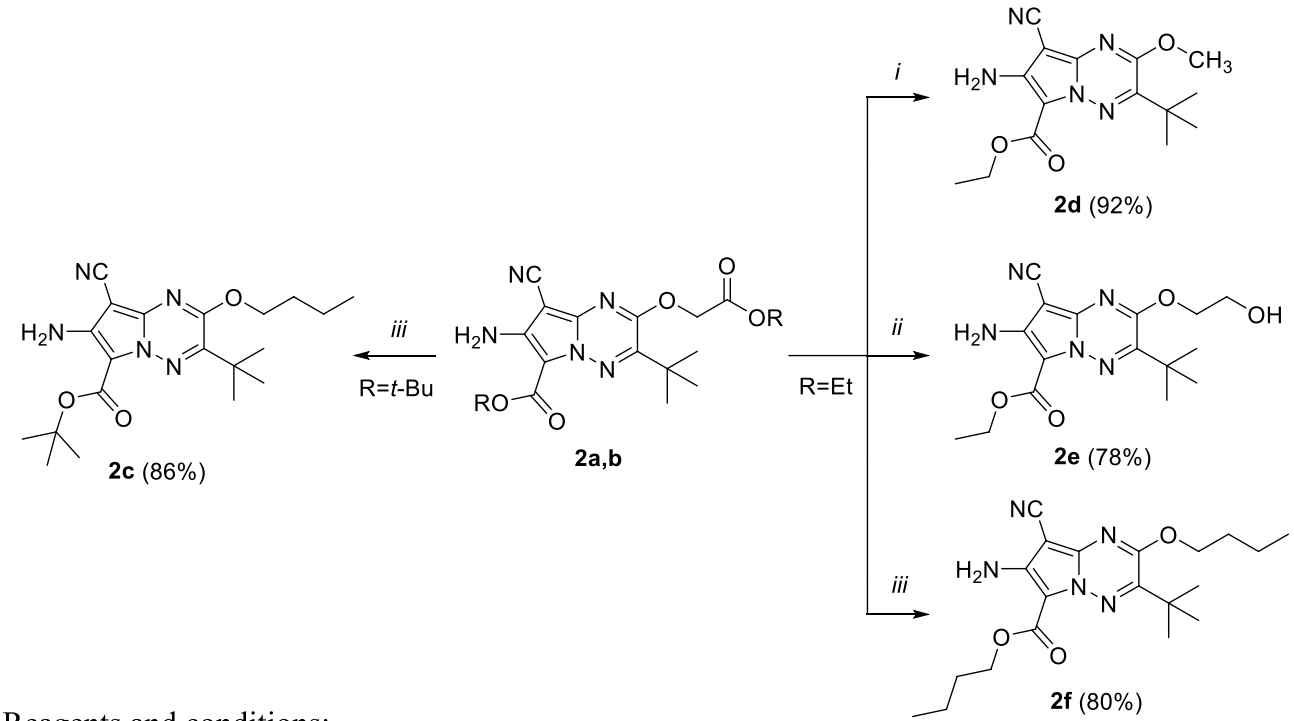

Reagents and conditions:

i: MeOH, K_2CO_3, Δ 40 min;

ii: Ethylene glycol, K_2CO_3, 100°C, 1 h;

iii: *n*-BuOH, K_2CO_3, Δ 5 h.

Scheme 2 Synthesis of compounds 2c–e

0.15 g (0.47 mmol, 92%), mp. 203–210 °C (decomp.). IR (KBr) ν = 3424, 3334 (NH_2), 2978, 2957, 2930, 2870 (CH), 2218 (CN), 1666 (C = O), 1623, 1598, 1554, 1524, 1481, 1450, 1402, 1375, 1310, 1259, 1202, 1150, 1122, 1051, 1024, 995, 931, 875, 835, 779, 766, 742, 716, 679, 633, 540, 513, 446, 429 cm^{-1}. ^1H NMR: (300 MHz, $CDCl_3$) δ 1.42 (t, J = 7.1 Hz, 3H, $OCH_2C\underline{H}_3$), 1.45 (s, 9H, Bu^t), 4.14 (s, 3H, OMe), 4.39 (q, J = 7.1 Hz, 2H, $OC\underline{H}_2CH_3$), 5.59 (s, 2H, $N\underline{H}_2$). $^{13}C\{^1H\}$ NMR: (APT, 126 MHz, $CDCl_3$) δ 14.47 ($OCH_2\underline{C}H_3$), 27.77 ($C(\underline{C}H_3)_3$), 37.38 ($\underline{C}(CH_3)_3$), 54.60 ($O\underline{C}H_3$), 59.99 ($O\underline{C}H_2CH_3$), 113.53 (CN), 99.82, 139.36, 148.02, 148.17, 155.08, 159.87, 161.12 (C(2), C(3), C(6), C(7), C(8), C(8a) and $\underline{C}O_2Et$). HRMS m/z ($I_{rel.}$ %) calculated: 318.1561 $[M+H]^+$, found: 318.1556 $[M+H]^+$ (100). Anal. calcd. for $C_{15}H_{19}N_5O_3$ (%): C, 56.77, H, 6.03, N, 22.07. Found (%): C, 56.81, H, 6.05, N, 22.03.

Ethyl 7-amino-3-*tert*-butyl-8-cyano-2-(2-hydroxyethoxy) pyrrolo[1,2-*b*][1,2,4]triazine-6-carboxylate (2e) Colorless crystals, yield 0.14 g (0.40 mmol, 78%), mp. 95–110 °C (decomp.). IR (KBr) ν 3421, 3331 (br., OH, NH_2), 2970, 2957, 2931 (CH), 2213 (CN), 1668, 1653 (C = O), 1623, 1597, 1548, 1522, 1482, 1463, 1410, 1382, 1369, 1348, 1311, 1261, 1202, 1158, 1131, 1097, 1049, 1026, 998, 905, 887, 824, 765, 724, 679, 632, 564, 532, 517, 426 cm^{-1}. ^1H NMR: (300 MHz, $CDCl_3$) δ 1.42 (t, J = 7.0 Hz, 3H, $OCH_2C\underline{H}_3$), 1.47 (s, 9H, Bu^t), 1.89 (br. s, 1H, OH), 4.08 (t, J = 4.6 Hz, 2H, $HOC\underline{H}_2$), 4.39 (q, J = 7.1 Hz, 2H, $OC\underline{H}_2CH_3$), 4.68 (t, J = 4.6 Hz, 2H, $OC\underline{H}_2CH_2OH$), 5.60 (s, 2H, $N\underline{H}_2$). $^{13}C\{^1H\}$ NMR: (APT, 75 MHz, $CDCl_3$, the signal of one of the quaternary carbons was not observed due to the broadening) δ 13.88 ($OCH_2\underline{C}H_3$), 27.26 ($C(\underline{C}H_3)_3$), 36.81 ($\underline{C}(CH_3)_3$), 59.05, 59.13 ($O\underline{C}H_2CH_2OH$), 68.55 ($O\underline{C}H_2CH_3$), 113.16 (CN), 98.96, 138.91, 147.45, 147.82, 154.13, 160.34 (C(2), C(3), C(6), C(7), C(8), C(8a) and $\underline{C}O_2Et$). HRMS m/z ($I_{rel.}$ %) calculated: 348.1666 $[M+H]^+$, found: 348.1657 $[M+H]^+$ (100). Anal. calcd. for $C_{16}H_{21}N_5O_4$ (%): C, 55.32, H, 6.09, N, 20.16. Found (%): C, 55.35, H, 6.04, N, 20.21.

Butyl 7-amino-2-butoxy-3-*tert*-butyl-8-cyanopyrrolo[1, 2-*b*][1,2,4]triazine-6-carboxylate (2f) Colorless crystals, yield 0.16 g (0.41 mmol, 80%), mp. 156–158 °C. IR (KBr) ν = 3421, 3329 (NH_2), 2994, 2957, 2932, 2870 (CH), 2216 (CN), 1655 (C = O), 1622, 1552, 1519, 1481, 1418, 1366, 1350, 1315, 1261, 1203, 1167, 1137, 1119, 1057, 1024, 1012, 973, 941, 901, 861, 845, 817, 781, 766, 752, 720, 682, 632, 566, 538, 507, 429 cm^{-1}. ^1H NMR: (300 MHz, $CDCl_3$) δ 0.97 (t, J = 7.1 Hz, 3H, $O(CH_2)_3C\underline{H}_3$), 1.02 (t, J = 7.1 Hz, 3H, $O(CH_2)_3C\underline{H}_3$), 1.45 (s, 9H, Bu^t), 1.47–1.57 (m, 4H, 2 $O(CH_2)_2C\underline{H}_2CH_3$), 1.72–1.91 (m, 4H, 2 $OCH_2C\underline{H}_2CH_2CH_3$), 4.34 (t, J = 7.1 Hz, 2H, $OC\underline{H}_2$), 4.54 (t, J = 7.1 Hz, 2H, $OC\underline{H}_2$), 5.59 (br. s, 2H, $N\underline{H}_2$). $^{13}C\{^1H\}$ NMR: (APT, 151 MHz, $CDCl_3$, the signals of the two quaternary carbons were not observed due to the broadening) δ 13.23 (2 $O(CH_2)_3\underline{C}H_3$, two signals overlapped), 18.85, 18.94 (2 $O(CH_2)_2\underline{C}H_2CH_3$), 27.34 ($C(\underline{C}H_3)_3$), 29.97, 30.38 (2 $OCH_2\underline{C}H_2CH_2CH_3$), 36.90 ($\underline{C}(CH_3)_3$), 63.47, 67.36 (2 $O\underline{C}H_2$), 113.17 (CN), 99.25, 139.04, 147.67, 154.30, 160.78 (C(2), C(3), C(6), C(7), C(8), C(8a) and $\underline{C}O_2Bu^n$). HRMS m/z ($I_{rel.}$ %) calculated: 388.2343 $[M+H]^+$, found: 388.2334 $[M+H]^+$ (100). Anal. calcd. for $C_{20}H_{29}N_5O_3$ (%): C, 61.99, H, 7.54, N, 18.07. Found (%): C, 61.96, H, 7.51, N, 18.06.

***tert*-Butyl 7-amino-2,3-di-*tert*-butyl-8-cyanopyrrolo[1,2-*b*] [1,2,4]triazine-6-carboxylate (4b)** Bu^tLi solution (1.7 M in *n*-pentane, 1.5 ml, 2.55 mmol) was added dropwise over 5 min to a cooled (–110 ÷ –105 °C) solution of compound **2b** (0.5 mmol) in 30 ml of dry THF, with vigorous stirring. After the addition was complete, the reaction mixture was further stirred at –100 for 20 min. Next, the cooling bath was removed, and 3 ml of a saturated KH_2PO_4/H_2O solution was added dropwise over 1 min. The resulting mixture was stirred for 30 min (the inner temperature reached 0 °C), quenched with H_2O (30 ml), EtOAc (30 ml), and heptane (20 ml). The organic phase was separated, washed with H_2O (1 × 50 ml), dried with anhydrous $MgSO_4$, and filtered. The solvents were removed in vacuo, and the residue was purified by column chromatography (eluted with EtOAc:heptane = 1:100–1:20) to give compound **4a**, bright yellow crystals (CCDC 2,055,900), yield 20 mg (0.06 mmol, 13%), mp. 140–150 °C (decomp., spectral and X-ray data coincided with those described in literature [19]), and compound **4b** as yellow crystals, yield 0.14 g (0.38 mmol, 75%), mp. 181–183 °C. IR (KBr) ν = 3431, 3321 (NH_2), 3051, 3031, 3006, 2982, 2965, 2930 (CH), 2227 (CN), 1661 (C = O), 1616, 1535, 1500, 1473, 1451, 1431, 1391, 1365, 1322, 1253, 1200, 1217, 1148, 1098, 1068, 1009, 924, 848, 825, 787, 767, 707, 692, 678, 621, 603, 515, 479, 430 cm^{-1}. ^1H NMR: (300 MHz, $CDCl_3$) δ 1.56, 1.59, 1.64 (3 s, 9H + 9H + 9H, 3 Bu^t), 5.75 (br. s, 2H, NH_2). ^{13}C NMR: (APT, 75 MHz, $CDCl_3$) δ 28.88, 31.70, 32.13 (3 $C(\underline{C}H_3)_3$), 40.31, 41.58 ((C(2), C(3))–$\underline{C}(CH_3)_3$), 69.46 (C(8)), 81.90 (O–$\underline{C}(CH_3)_3$), 113.75 (CN), 101.69, 136.28, 149.48, 154.99, 160.81, 160.87 (C(2), C(3), C(6), C(7), C(8a) and $\underline{C}O_2Bu^t$). HRMS m/z ($I_{rel.}$ %) calculated: 394.2213 $[M+Na]^+$, found: 394.2206 $[M+Na]^+$ (100). Anal. calcd. for $C_{20}H_{29}N_5O_2$ (%): C, 64.66, H, 7.87, N, 18.85. Found (%): C, 64.60, H, 7.92, N, 18.89.

***tert*-Butyl 7-amino-2,2,3-tri-*tert*-butyl-8-cyano-1,2-dihydropyrrolo[1,2-*b*][1,2,4]triazine-6-carboxylate (5)** Bu^tLi solution (1.7 M in *n*-pentane, 4.5 ml, 7.65 mmol)

was added dropwise over 5 min to a cooled (–110÷–105 °C) solution of compound **4b** (0.5 mmol) in 30 ml of dry THF, with vigorous stirring. After the addition was complete, the reaction mixture was further stirred at –85÷–80 °C for 30 min. Next, the cooling bath was removed, and 3 ml of a saturated KH_2PO_4/H_2O solution was added dropwise over 1 min. The resulting mixture was stirred for 30 min (the inner temperature reached 0 °C), and the product was isolated by chromatography, analogously as described above (for **4a,b**). Compound **5**, colorless crystals, yield 0.18 g (0.42 mmol, 84%), mp. 140–150 °C (decomp.). IR (KBr) $\nu = 3477$, 3360, 3343 (NH), 3031, 2967, 2928 (CH), 2206 (CN), 1646 (C = O), 1624, 1607, 1539, 1507, 1475, 1457, 1420, 1396, 1358, 1305, 1262, 1221, 1185, 1145, 1088, 1059, 1030, 985, 943, 920, 883, 850, 819, 785, 760, 680, 663, 635, 598, 517, 490, 461, 425 cm^{-1}. ^1H NMR: ($^1H/^1H$–^{13}C HMBC, 600 MHz, $CDCl_3$) δ 1.23 (s, 18H, C(2)$(Bu^t)_2$), 1.56 (s, 9H, C(3)Bu^t), 1.58 (s, 9H, OBu^t), 5.10 (br. s, 1H, N(1)–H), 5.22 (br. s, 2H, NH_2). ^{13}C NMR: (75 MHz APT/151 MHz ^1H–^{13}C HMBC, $CDCl_3$) δ 29.22 (OC($\underline{C}H_3)_3$), 29.36 (C(2)($C(\underline{C}H_3)_3)_2$), 34.45 (C(3)$C(\underline{C}H_3)_3$), 43.34 (C(3)$\underline{C}(CH_3)_3$), 43.78 (C(2)($\underline{C}(CH_3)_3)_2$), 59.98 (C(8)), 71.88 (C(2)), 79.91 (O–$\underline{C}(CH_3)_3$, 114.66 (CN), 98.24, 145.52 (C(6), C(7)), 138.39 (C(8a)), 158.55 (C(3)), 161.25 ($\underline{C}O_2Bu^t$). HRMS *m/z* ($I_{rel.}$ %) calculated: 452.2996 $[M + Na]^+$, found: 452.2986 $[M + Na]^+$ (100). Anal. calcd. for $C_{24}H_{39}N_5O_2$ (%): C, 67.10, H, 9.15, N, 16.30. Found (%): C, 67.16, H, 9.13, N, 16.28.

For X-ray single crystal studies, all compounds were recrystallized by slow solvent evaporation at r.t. from nearly saturated solutions in ethyl acetate/heptane mixture (2:1 v/v).

X-ray data collection and refinement

X-ray diffraction data were collected at 100 K (compounds **2a,e,f, 3, 4b, 5**) or 250 K (compound **2d**) on a Bruker Quest D8 diffractometer equipped with a Photon-III area-detector (graphite monochromator, shutterless φ-, and ω-scan technique), using Mo K_α-radiation (0.71073 Å). The intensity data were integrated by the SAINT program [20] and were corrected for absorption and decay using SADABS [21]. The structures were solved by direct methods using SHELXT [22] and refined on F^2 using SHELXL-2018 [23]. All non-hydrogen atoms were refined with individual anisotropic displacement parameters. Locations of H-atoms of amino (H6A and H6B for **2a,f** and **3**, H6A, H6B, H6C, and H6D for **2d**, H4A, H4B, H9A, and H9B for **2e**, H2A and H2B for **4b**, H1, H4A, and H4B for **5**) and hydroxy (H2 and H6 for **2e**) groups were found from the electron density-difference map; these atoms were refined with individual isotropic displacement parameters. Positions of atoms H6A and H6B in **3** were restrained at the distance of 0.85(3)Å from N6. All other hydrogen atoms were placed in ideal calculated positions and refined as riding atoms with relative isotropic displacement parameters. A rotating group model was applied for methyl groups in **5**.

The SHELXTL program suite [20] was used for molecular graphics. Displacement ellipsoids are set to the 50% probability level on all figures below (see Electronic Supplementary Material (ESM) for more details on X-ray data collection and refinement).

Crystal data, data collection, and structure refinement details for **2a,d–f** and **3, 4b, 5** are summarized in Table 1 and Table 2. Crystal data for compounds **2c** (CCDC 2,017,998) and **4a** (CCDC 2,055,900) have been previously described in literature [16, 19]. Bond distances and angles, as well as additional *ORTEP* drawings, are presented in ESM for this paper. The structures **2a,d–f** and **3, 4b, 5** have been deposited at the Cambridge Crystallographic Data Center with the reference CCDC numbers 2024439, 2,024,440, 2,077,346, 2,077,350–2,077,352, and 2,098,491; they also contain the supplementary crystallographic data. These data can be obtained free of charge from the CCDC via http://www.ccdc.cam.ac.uk/data_request/cif.

A geometry optimization was calculated using GAUSSIAN 09 software [24] with the B3LYP/6-31G(d) basis set at the level of DFT theory. Hirshfeld surface analysis was calculated using CrystalExplorer 21.5 [25] and comprised 2D (two-dimensional) fingerprint plots and d_{norm} surface plots [26]. The electrostatic potentials were mapped on the Hirshfeld surfaces using the B3LYP/6-31G(d) basis set using TONTO computational package integrated into CrystalExplorer software [27]. The crystallographic information files (CIF) of the compounds **2a, 2e, 3, 4a, 4b,** and **5** were used as input for the analysis.

Results and discussion

Synthesis

The starting pyrrolotriazines 2a,b were synthesized by *N,O*-bis-alkylation and Thorpe-Ziegler 5-*exo*-dig type cyclizations [17] of 2-(6-*tert*-butyl-5-oxo-4,5-dihydro-1,2,4-triazin-3(2*H*)-ylidene)malononitrile 1 [18] with bromoacetic esters in the presence of potassium hydroxide (Scheme 1). Compound 3 was synthesized analogously, by treatment of 1 with isopropyl (*p*-bromomethyl)benzoate; this reagent also has the ability to stabilize the negative charge at the methylene moiety due to the π-conjugation [16, 28] with the carbonyl group in *p*-position. It is worth mentioning that an application of less hindered ethyl (*p*-bromomethyl)benzoate or

Table 1 Crystal data, data collection, and structure refinement for compounds **2a**,**d–f**

Compound	2a	2d	2e	2f
Formula	$C_{18}H_{23}N_5O_5$	$C_{15}H_{19}N_5O_3$	$C_{16}H_{21}N_5O_4$	$C_{20}H_{29}N_5O_3$
M_r	389.41	317.35	347.38	387.48
Crystal system	Triclinic	Triclinic	Monoclinic	Monoclinic
Space group	$P\bar{1}$	$P\bar{1}$	Cc	$P2_{1/c}$
Unit cell dimensions				
a (Å)	9.2033(2)	10.7314(7)	24.4431(7)	13.9557(4)
b (Å)	10.0079(3)	12.7659(8)	10.9353(3)	9.4756(3)
c (Å)	12.1067(3)	13.3259(9)	16.8945(9)	16.8243(5)
β (°)	80.2327(10)	75.9445(17)	129.5147(6)	107.7795(8)
Volume, Å^3	972.30(4)	1717.60(19)	3483.7(2)	2118.56(11)
Z	2	4	8	4
Calcd. density (g/cm^3)	1.330	1.227	1.325	1.215
μ (mm^{-1})	0.099	0.088	0.098	0.084
F(000)	412	672	1472	832
Crystal size (mm)	0.49×0.36×0.067	0.30×0.16×0.08	0.40×0.36×0.21	0.28×0.25×0.14
Θ range (°)	2.300 to 32.048	2.455 to 29.999	2.153 to 31.993	2.497 to 30.000
Complentess to Θ_{max}	0.999	0.999	1.000	1.000
Index ranges	$-13<=h<=13$ $-14<=k<=14$ $-18<=l<=18$	$-15<=h<=15$ $-17<=k<=17$ $-18<=l<=18$	$-36<=h<=36$ $-16<=k<=16$ $-25<=l<=25$	$-19<=h<=19$ $-13<=k<=13$ $-23<=l<=23$
Reflections				
Measured	97,812	56,157	91,179	50,206
Independent [R_{int}]	6760 [0.0322]	9996 [0.1108]	12,060 [0.0528]	6180 [0.0818]
Observed [$I>2\sigma(I)$]	6004	3882	10,371	4227
Parameters, restraints	266, 0	454, 3	483, 2	266, 0
R1, wR2 [$I>2\sigma(I)$]	0.0365, 0.0961	0.0770, 0.1586	0.0469, 0.1113	0.0637, 0.1166
R1, wR2 (all data)	0.0420, 0.1011	0.2076, 0.2290	0.0600, 0.1221	0.1046, 0.1364
GooF on F^2	1.037	1.025	1.032	1.065
$\Delta\rho_{max}$, $\Delta\rho_{min}$ (e Å^{-3})	0.489, −0.275	0.234, −0.201	0.529, −0.309	0.247, −0.326
CCDC number	2024439	2077351	2077350	2077352

p-nitrobenzyl bromide led to resinification, presumably, due to the ease of competing condensations with formed amino groups.

Nucleophilic heteroaromatic substitution [15, 29] of the C2-OCH_2CO_2Et group in 2a with methanol or ethylene glycol proceeded on heating in the presence of a catalytic amount of potassium carbonate, to give compounds 2d and 2e, respectively (Scheme 2). The process probably involves coordination of a metal cation [30], as no reaction was observed when K_2CO_3 was replaced with triethylamine. In the case of *n*-BuOH, a transesterification [31] of the C6-carboxyethyl group to give the corresponding *n*-butyl ester became the main competing process, which led to isolation of butyl 7-amino-2-butoxy-3-*tert*-butyl-8-cyanopyrrolo[1,2-*b*][1,2,4]triazine-6-carboxylate 2f in good yield (Scheme 2).

tert-Butyl carboxylate 2b was significantly more stable towards transesterification and reacted with *n*-BuOH/K_2CO_3 under analogous conditions to afford the expected compound 2c (Scheme 2) [16]. Heterocycle 2b also reacted with *t*-BuLi at low temperature (THF, –100 °C) to selectively give the aromatic 2,3-di-*tert*-butyl pyrrolotriazine 4b, along with a small amount of by-product 4a as a result of hydride transfer reduction [32, 33] (Scheme 3). XRD data for 2c and 4a were previously described in literature [16, 19]. On treatment with excess *t*-BuLi, 4b afforded the sterically hindered non-conjugated *tert*-butyl 7-amino-2,2,3-tri-*tert*-butyl-8-cyano-1,2-dihydropyrrolo[1,2-*b*]

Table 2 Crystal data, data collection, and structure refinement for compounds **3**, **4b**, **5**

Compound	**3**	**4b**	**5**
Formula	$C_{27}H_{33}N_5O_5$	$C_{20}H_{29}N_5O_2$	$C_{24}H_{39}N_5O_2$
M_r	507.58	371.48	429.60
Crystal system	Triclinic	Monoclinic	Monoclinic
Space group	$P\,\overline{1}$	$P2_{1/c}$	$P2_{1/n}$
Unit cell dimensions			
a (Å)	6.5352(2)	9.2224(2)	13.5941(6)
b (Å)	11.5286(4)	12.0168(3)	12.2011(5)
c (Å)	18.2987(7)	18.8805(4)	14.7166(6)
β (°)	94.5953(10)	97.7864(6)	102.9960(10)
Volume, Å^3	1325.39(8)	2073.12(8)	2378.42(17)
Z	2	4	4
Calcd. density (g/cm^3)	1.272	1.190	1.200
μ (mm^{-1})	0.089	0.079	0.078
F(000)	540	800	936
Crystal size (mm)	0.19 × 0.03 × 0.02	0.48 × 0.43 × 0.24	0.47 × 0.38 × 0.25
Θ range (°)	2.255 to 34.986	2.760 to 35.008	2.192 to 33.176
Complentess to Θ_{max}	0.997	0.998	0.985
Index ranges	$-10<=h<=10$ $-18<=k<=18$ $-29<=l<=29$	$-14<=h<=13$ $-19<=k<=19$ $-30<=l<=30$	$-20<=h<=20$ $-18<=k<=18$ $-22<=l<=22$
Reflections			
Measured	64,206	68,972	60,463
Independent [R_{int}]	11,655 [0.0960]	9131 [0.0337]	8943 [0.0807]
Observed [$I>2\sigma(I)$]	5283	7517	6136
Parameters, restraints	483, 70	261, 0	304, 0
R1, wR2 [$I>2\sigma(I)$]	0.0732, 0.1572	0.0453, 0.1180	0.0592, 0.1335
R1, wR2 (all data)	0.1793, 0.2028	0.0577, 0.1281	0.0984, 0.1566
GooF on F^2	1.008	1.023	1.033
$\Delta\rho_{max}$, $\Delta\rho_{min}$ (e Å^{-3})	0.345, −0.389	0.469, −0.296	0.523, −0.287
CCDC number	2024440	2077346	2098491

[1,2,4]triazine-6-carboxylate 5. An application of *n*-BuLi or Grignard reagents gave no reaction or resinification at elevated temperatures. It is worth mentioning that the mechanism of *t*-BuLi addition (to give 4b and 5) may differ from simple nucleophilic heteroaromatic substitution, as it may involve single electron transfer and further recombination of radicals [33]. Crystals were successfully grown for the novel compounds 2a,d–f and 3, 4b, 5 and X-ray diffraction analyses were carried out.

Crystal structure discussion

Molecular structure description

The series of synthesized 7-amino-3-*tert*-butyl-8-cyano-2-alkoxypyrrolo[1,2-*b*][1,2,4]triazine-6-(*p*-phenylene) carboxylates 2a,c–f and 3 crystallize from ethyl acetate/heptane (2:1) mixture in triclinic (*P I* for 2a,d and 3) or monoclinic (*Cc* for 2e, $P2_1/c$ for 2f, and $P2_1/n$ for 2c) crystal systems without inclusion of solvent molecules into the crystal lattice. Compounds 4a,b, and 5 were crystallized also in monoclinic crystal system (the $P2_1/n$ space groups for 4a and 5, and $P2_1/c$ for 4b, respectively). Results of X-ray diffraction studies for novel compounds 2a,d–f, 3 (Figs. 1, 2, and 3) and 4b, 5 (Fig. 4) are presented in Tables 3, 4, 5, and 6.

The isolated 2-alkoxy substituted compounds 2a,c–f, 3 (Figs. 1, 2, and 3) possess aromatic pyrrolotriazine system fully conjugated with the exocyclic amino, cyano, and ester groups; the notable exception is 6-arylsubstituted compound 3 (Fig. 1, ESM Fig. S31), which features non-coplanar hetaryl and disordered phenyl moieties (C7–C6–C20–C25A, θ = −31.8(3)°, C7–C6–C20–C25B, θ = 28.0(3)°). The C8–C8a bond in 3 is 0.017–0.023 Å shorter than in 2a,c–f,

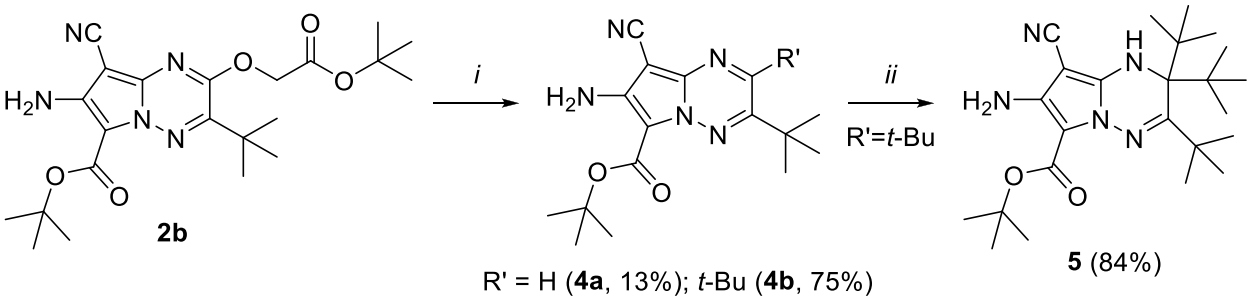

Reagents and conditions:

i: *t*-BuLi, THF, –100°C, 20 min;

ii: *t*-BuLi, THF, –80°C, 30 min.

Scheme 3 Synthesis of compounds **2b, 4a,b, and 5**

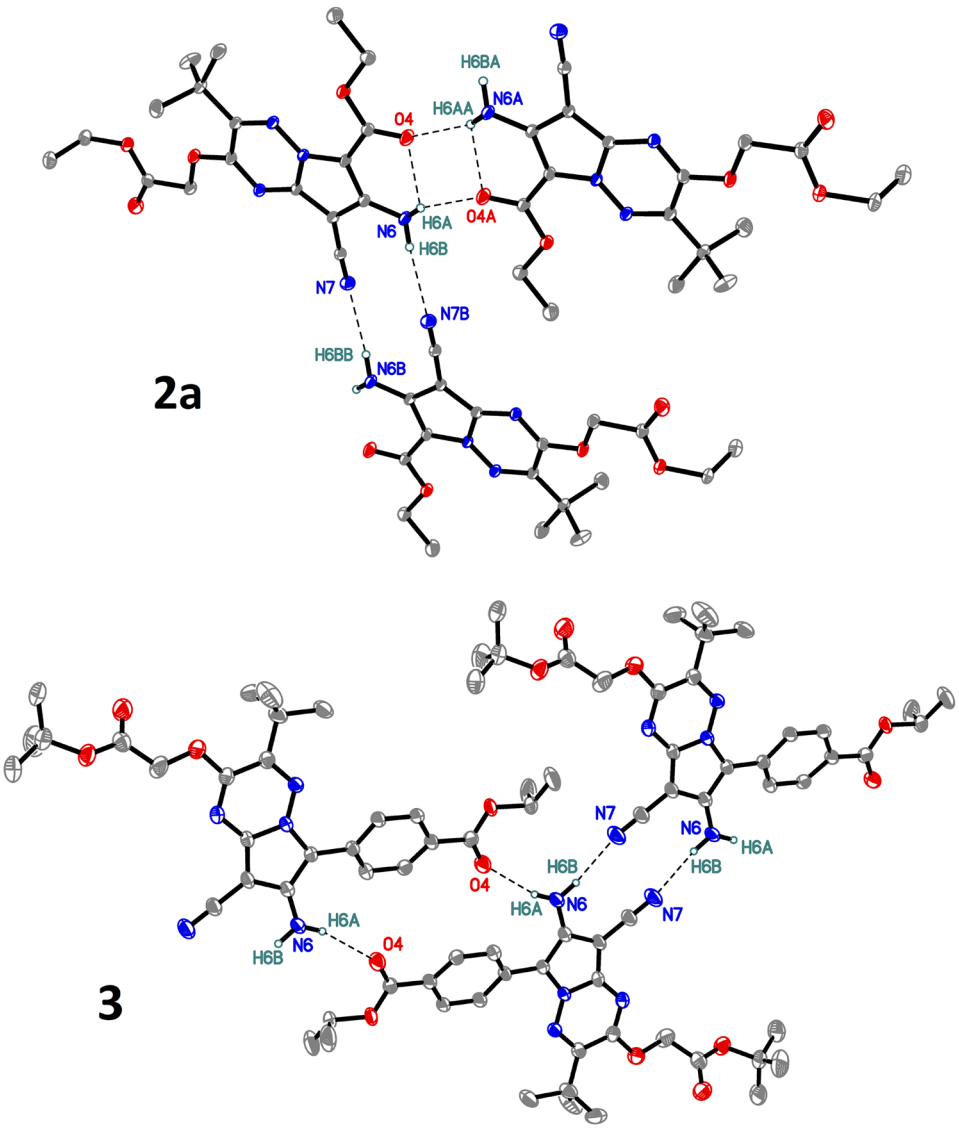

Fig. 1 Molecular structures of 2a and 3. H-atoms of alkyl and aryl groups are omitted; displacement ellipsoids are shown at the 50% probability level

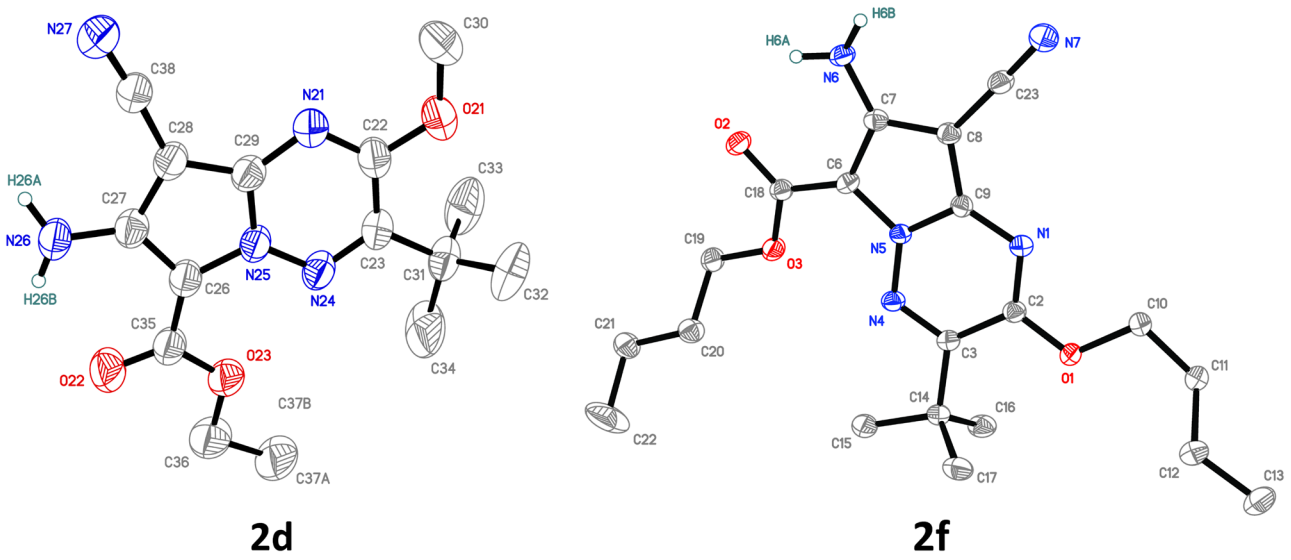

Fig. 2 Molecular structures of **2d** and **2f**. H-atoms of alkyl groups are omitted; displacement ellipsoids are shown at the 50% probability level

which also demonstrated the somewhat different π-electron density distribution in the system. Other heterocyclic bond differences within the series are subtle and typically lied within 0.01 Å.

On switching from oxygen in the C2 ring position of 2a,c–f and 3 to *tert*-butyl group in compound 4b (Fig. 4), a marked increase in the lengths of all the 1,2,4-triazine bonds non-shared with the pyrrole N1–C2, C2–C3 and C3–N4 by 0.02–0.04 Å was observed, together with a slight decrease of the shared bonds N1–C8a, N4–N5 by ~ 0.02 Å, which was apparently the result of the steric repulsion between the bulky *t*-Bu substituents in the nearby positions. On the other hand, compound 4a non-substituted in C2 position showed C2–C3 bond lengths considerably shortened (by 0.03–0.05 Å) when compared with its closest analogs 2c and 4b. Triazine ring strain was substantiated by the practically

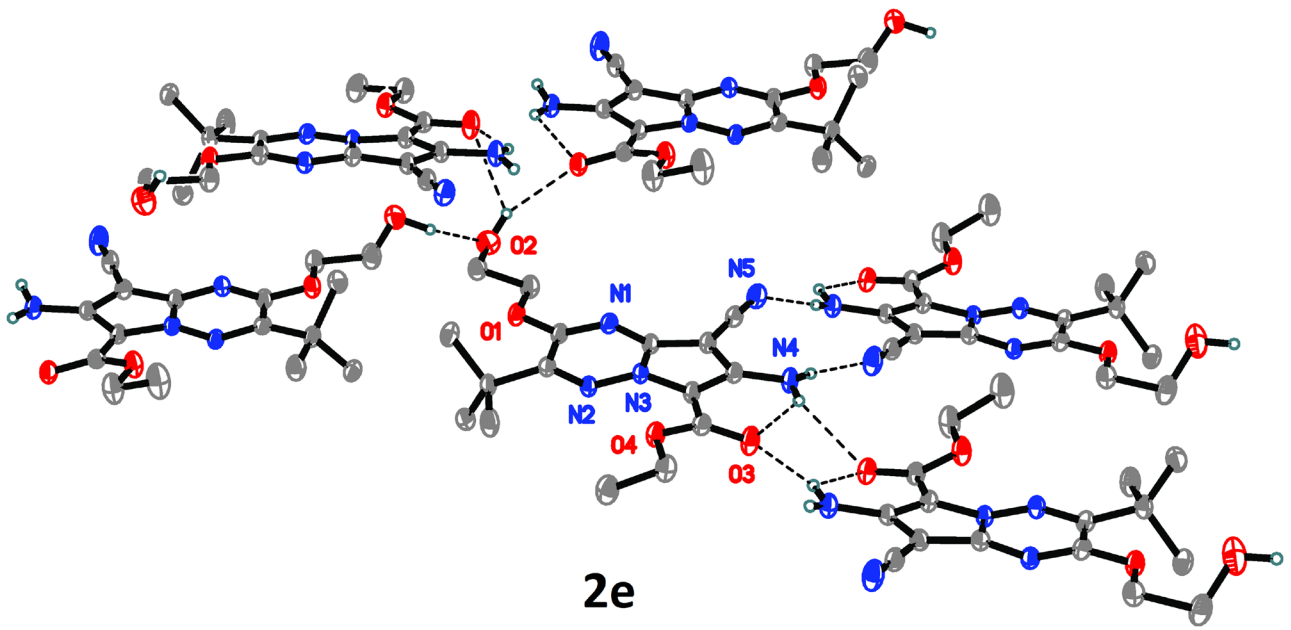

Fig. 3 Packing of compound **2e** in a single crystal. H-atoms of alkyl groups are omitted; displacement ellipsoids are shown at the 50% probability level

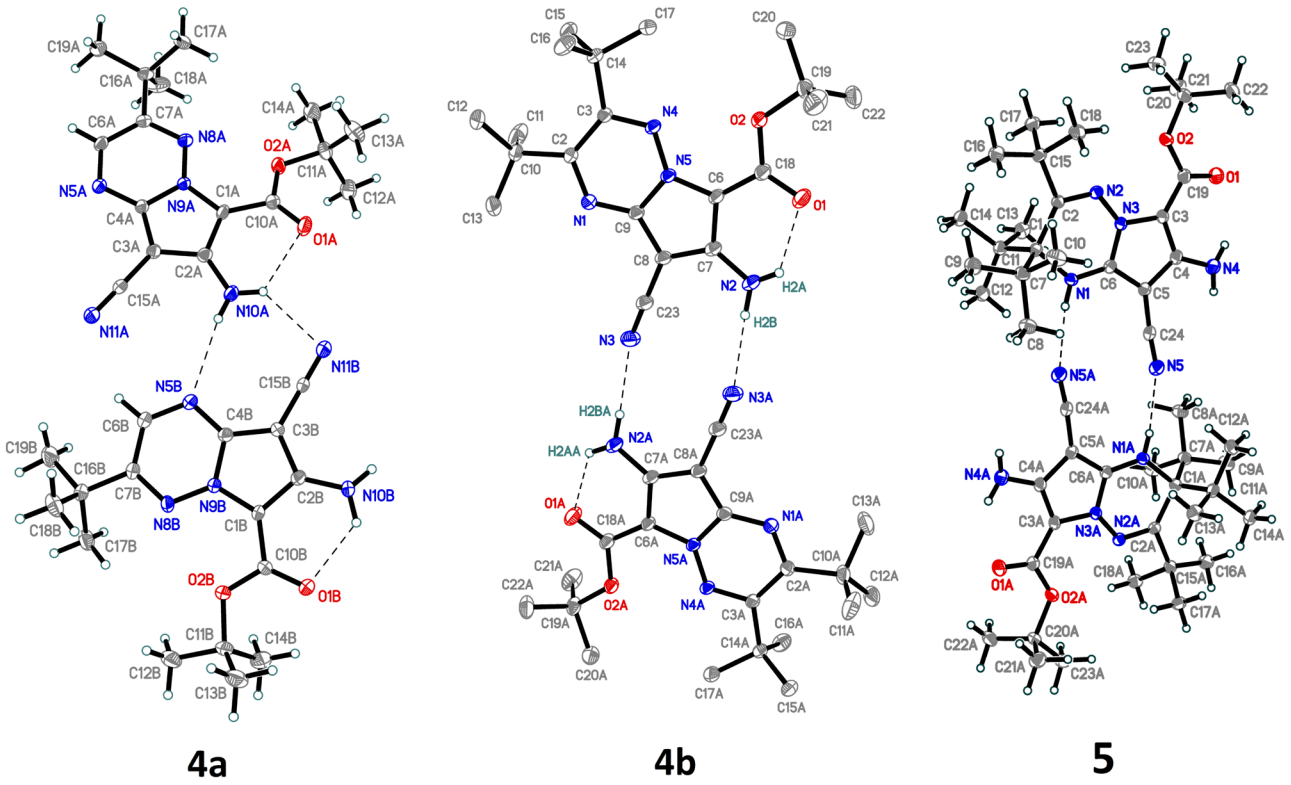

Fig. 4 Molecular structures of **4a, 4b,** and **5**. H-atoms of alkyl groups in **4b** are omitted; displacement ellipsoids are shown at the 50% probability level

planar conformation of the bicycle 4b in the single crystal: N1–C2–C3–N4 and Me_3C–C2–C3–CMe_3, θ = −3.0(1)° and 3.7(1)°, respectively. Six-membered ring in compound 5, despite also being nearly planar (with the deviations of about 3–8°), is non-aromatic, as evidenced from the alternating single and double bond lengths: N1–C2, C3–N4 = 1.4979(16) and 1.2882(16) Å, respectively for 5, and within 1.30–1.33 Å for other analyzed compounds 2a,c–f, 3, and 4a,b.

The C6–CO_2Alk distance arises with increase in the size of the Alk substituent: from 1.427–1.439 (Alk = Et, in **2a,e,d**), 1.437 Å (Alk = *n*-Bu, in **2f**) to 1.448–1.457 Å (Alk = *t*-Bu, in **2c** and **4a,b**). The C2–O in **3** is notably longer

Table 3 Selected bond distances in **2a,c-f** and **3** (Å)

Bond	2a	2e	2d	3	2f	2c
N1–C2	1.3101(9)	1.309(3)	1.311(4)	1.298(2)	1.311(2)	1.3108(17)
N1–C8a	1.3484(9)	1.346(3)	1.350(3)	1.342(2)	1.347(2)	1.3479(17)
C2–C3	1.4478(10)	1.450(3)	1.427(5)	1.444(2)	1.449(2)	1.4498(19)
C3–N4	1.3110(9)	1.310(3)	1.314(4)	1.315(2)	1.311(2)	1.3112(17)
N4–N5	1.3414(8)	1.344(2)	1.353(3)	1.3475(19)	1.3444(18)	1.3449(15)
N5–C6	1.3991(9)	1.404(3)	1.403(3)	1.392(2)	1.405(2)	1.4039(17)
N5–C8a	1.3783(9)	1.377(3)	1.364(4)	1.3885(19)	1.373(2)	1.3803(17)
C6–C7	1.4041(10)	1.401(3)	1.386(4)	1.406(2)	1.397(2)	1.3953(19)
C7–C8	1.4275(10)	1.431(3)	1.427(4)	1.425(2)	1.425(2)	1.4289(19)
C8–C8a	1.3987(9)	1.397(3)	1.394(4)	1.377(2)	1.399(2)	1.4002(19)
C8–CN	1.4126(10)	1.414(3)	1.405(4)	1.416(2)	1.412(2)	1.417(2)
C7–NH_2	1.3527(9)	1.347(3)	1.349(3)	1.359(2)	1.360(2)	1.3565(18)
C2–O	1.3371(8)	1.338(2)	1.340(3)	1.356(2)	1.334(2)	1.3360(16)
C6–CO, C_{Ar}	1.4384(10)	1.439(3)	1.427(4)	1.458(2)	1.437(2)	1.4479(19)

Table 4 Selected experimental and calculated (B3LYP/6-31G(d), gas phase) bond distances in **4a,b** and **5** (Å)

Bond	4a (X-ray)	4b (DFT)	4b (X-ray)	5 (DFT)	5 (X-ray)
N1–C2	1.320(3), 1.328(3)	1.3442	1.3255(9)	1.4878	1.4979(16)
N1–C8a	1.346(3), 1.335(3)	1.3336	1.3289(10)	1.3430	1.3365(16)
C2–C3	1.416(3), 1.415(3)	1.4673	1.4658(10)	1.6027	1.5847(16)
C3–N4	1.325(3), 1.328(3)	1.3480	1.3288(9)	1.2923	1.2882(16)
N4–N5	1.342(3)	1.3395	1.3314(8)	1.3521	1.3574(14)
N5–C6	1.391(3), 1.390(3)	1.3992	1.3931(9)	1.4317	1.4240(16)
N5–C8a	1.388(3), 1.396(3)	1.4052	1.3733(10)	1.3509	1.3460(15)
C6–C7	1.406(3), 1.411(3)	1.4265	1.4120(10)	1.4007	1.3859(17)
C7–C8	1.421(3), 1.419(3)	1.4292	1.4168(11)	1.4409	1.4343(17)
C8–C8a	1.397(3)	1.4050	1.4009(10)	1.4014	1.4076(17)
C8–CN	1.414(3)	1.4065	1.4110(11)	1.4074	1.4094(17)
C7–NH_2	1.345(3)	1.3506	1.3500(10)	1.3541	1.3626(17)
C2–O, $C_{t\text{-Bu}}$	-	1.5596	1.5510(11)	1.6230, 1.6358	1.6080(18), 1.6168(17)
C6–CO	1.457(3), 1.449(3)	1.4411	1.4478(11)	1.4376	1.4372(17)

Table 5 Intermolecular hydrogen-bond parameters (Å, °) in **2a, 2e,** and **3**

Compound	*D*—H···*A*	*D*—H (Å)	H···*A* (Å)	*D*···*A* (Å)	*D*—H···*A* (°)
2a	N(6)—H(6A)···O(4)^{i}	0.863(13)	2.225(14)	3.0379(9)	156.8(12)
	N(6)—H(6B)···N(7)^{ii}	0.882(14)	2.294(15)	3.1648(10)	169.3(13)
2e	O(6)—H(6)···O(2)	1.00(5)	1.82(5)	2.785(3)	162(5)
	O(2)—H(2)···O(3)^{iii}	0.87(4)	2.47(4)	3.080(3)	127(3)
	O(2)—H(2)···O(7)^{iv}	0.87(4)	2.31(4)	3.127(3)	155(4)
	N(4)—H(4A)···O(7)^{v}	0.78(3)	2.48(3)	3.192(3)	151(3)
	N(9)—H(9B)···O(3)^{vi}	0.89(4)	2.19(4)	3.046(3)	160(3)
	N(4)—H(4B)···N(10)^{vii}	0.84(4)	2.18(4)	3.010(3)	172(3)
	N(9)—H(9A)···N(5)^{viii}	0.85(3)	2.32(3)	3.151(3)	170(3)
3	N(6)—H(6A)···O(4A)^{ix}	0.86(2)	2.18(2)	3.020(3)	164(3)
	N(6)—H(6A)···O(4B)^{ix}	0.86(2)	2.31(3)	3.078(3)	149(3)
	N(6)—H(6B)···N(7)^{x}	0.901(19)	2.219(19)	3.106(2)	168(2)

Symmetry codes: (i) $-x+1,-y+2,-z$; (ii) $-x+2,-y+1,-z$; (iii) $x,-y+1,z-1/2$; (iv) $x+1/2,y-1/2,z+1$; (v) $x+1/2,-y+3/2,z+3/2$; (vi) $x-1/2,-y+3/2,z-3/2$; (vii) $x+1/2,-y+1/2,z+3/2$; (viii) $x-1/2,-y+1/2,z-3/2$; (ix) $-x+2,-y+1,-z+1$; (x) $-x,-y,-z+1$

Table 6 Intermolecular hydrogen-bond parameters (Å, °) in **2d, 2f, 2c, 4a, 4b**, and **5**

Compound	*D*—H···*A*	*D*—H (Å)	H···*A* (Å)	*D*···*A* (Å)	*D*—H···*A* (°)
2d	N(6)—H(6A)···N(27)^{i}	0.89(3)	2.22(3)	3.098(4)	169(3)
	N(26)—H(26A)···N(7)^{ii}	0.87(3)	2.41(3)	3.252(4)	164(2)
	N(6)—H(6B)···O(22)^{iii}	0.87(3)	2.25(3)	3.016(3)	147(3)
	N(26)—H(26B)···O(2)^{iv}	0.88(3)	2.31(4)	3.098(3)	150(3)
2f	N(6)—H(6A)···N(7)^{v}	0.87(3)	2.68(2)	3.358(2)	136(2)
	N(6)—H(6B)···O(2)^{vi}	0.92(2)	2.05(2)	2.960(2)	168(2)
2c	N(2)—H(2B)···N(3)^{vii}	0.87(2)	2.31(2)	3.1177(18)	153.6(17)
4a	N(10A)—H(3)···N(11B)	0.88(3)	2.39(2)	3.048(3)	132(2)
	N(10B)—H(1)···N(11A)^{viii}	0.91(4)	2.50(3)	3.162(3)	130(3)
	N(10A)—H(2)···N(5B)	0.85(3)	2.47(3)	3.306(3)	168(3)
	N(10B)—H(10)···N(5A)^{viii}	0.86(3)	2.28(3)	3.143(3)	172(2)
4b	N(2)—H(2B)···N(3)^{ix}	0.878(14)	2.160(14)	3.0374(10)	177.7(13)
5	N(1)—H(1)···N(5)^{x}	0.845(17)	2.294(17)	3.1190(15)	165.3(16)
	N(4)—H(2)···O(1)^{xi}	0.876(19)	2.29(2)	2.9556(16)	132.9(16)

Symmetry codes: (i) $x+1,y,z-1$; (ii) $x-1,y,z+1$; (iii) $x,y,z-1$; (iv) $x,y,z+1$; (v) $-x+1,y+1/2,-z+3/2$; (vi) $-x+1,y-1/2,-z+3/2$; (vii) $-x+1,-y,-z+1$; (viii) $x-1,y,z$; (ix) $-x+2,-y+1,-z+1$; (x) $-x,-y+1,-z+1$; (xi) $-x+1,-y+1,-z+1$

(by 0.016–0.022 Å) than the corresponding bond in other compounds; this may also be due to the bulky exocyclic substituent (CH_2Boc vs Me, *n*-Bu and CH_2CO_2Et). A sharp increase in the lengths of the C2–C_{Bu} and C3–C_{Bu} bonds on switching from **2a,c–f, 3, 4a** (1.52–1.53 Å) to compounds **4b** (1.55 Å) and **5** (up to 1.6168(17) Å) is no doubt due to the rising steric hindrance [34, 35]. According to the NMR (^{1}H and ^{13}C at 600 and 151 MHz, respectively), *t*-Bu groups in the C2 ring position of **5** are magnetically equivalent; however, the two Me_3C–C2 bonds differ for about 0.01 Å and ~ 2–3° (∠ N1–C2–CMe_3 and C3–C2–CMe_3).

Non-valence interactions

The crystals of the studied compounds are found to be rich in hydrogen bonding, which changes with the substitution pattern in heterocyclic nucleus. For instance, each molecule of compound **2a** forms intramolecular H-bonds between one of the hydrogens of an amino group and the carbonyl oxygen in the C6 ring position, as well as the intermolecular N—H···O = C(OEt) bonds with the nearby molecule; the dimers form infinite nearly planar chains along the *a* axes via H-bonding between the C8-nitrile nitrogen and the second hydrogen atom of C7–NH_2 (Fig. 1 and Table 5). The chains are held together by non-covalent π-π interactions, the intercentroid distances between stacking rings are in range 3.674 ÷ 3.787 Å. The *p*-phenylene linker in compound **3** eliminated any intramolecular H-bonds; however, the same tendency to form hydrogen bonds between amino-groups and the ester carbonyls of the nearby molecules as well as N—H···N≡C along the *b* axes is observed (Fig. 1). The presence of an additional hydroxyl moiety in the side chain of compound **2e** allowed the construction of 3D H-bonded infinite framework (Fig. 3). Thus, two nearby molecules of **2e** form the shortest hydrogen bonds within the series, with the distance O(6)—H(6)···O(2) = 2.785(3) Å, while the non-valence interactions between layers are provided by the O(2)H(2)···$[O=C(OEt)]_2$ H-bonds (Table 5).

The nature and amount of the observed hydrogen bonds were also strongly dependent upon the size of the substituents. Thus, compound **2d** form two types of H-bonds: C7–NH···O = C(OEt)–C6 and C7–NH···N≡C–C8 which parameters resemble that of **2a,e** (Table 6). On switching to **2f**, the bulkier C6–CO_2n-Bu group considerably hindered the formation of NH···N≡C hydrogen bonds (∠ N(6)–H(6A)···N(7) = 136(2)°), while change to C6–Boc in **2c** and **4a,b** completely eliminated any intermolecular C7–NH···O non-valence interactions (Fig. 4 and Table 6). However, this tendency is not observed in the case of compound **5**, probably due to the re-distribution of the π-density in the pyrrole and non-conjugated triazine rings. The latter compound showed intermolecular C7–NH_2···O = C hydrogen bonds of the same type as in crystals of **2a,e,d**, while the infinite chains along the *a* axes were formed via H-bonding between the C8-C≡N and N2–H (Fig. 4). Sterically accessible triazine ring in **4a** was also involved in the intermolecular H-bonding of the type N2···NH_2···N≡C (Fig. 4 and Table 6) and C2–H···N≡C (C2···N = 3.225(3) Å, ∠ C2–H···N = 145.5°).

DFT calculations

Geometries of compounds **4b** and **5** extracted from the XRD data were optimized at the B3LYP/6-31G(d) level of theory. The calculated structures in the gas phase (Fig. 5 and Table 4) exhibited notably elongated lengths of N1–C2, C3–N4, N5–C8a (1.4052 vs 1.3733(10) Å), and C6–C7 bonds for **4b**, and C2–C3, C2–$C_{t\text{-Bu}}$ (1.6358 vs 1.6168(17) Å) for **5**. The other bond differences were subtle and typically lied within 0.01 Å, and good correlations between the calculated and experimental values were obtained for N1–C8a, N4–N5, N5–C6, C8–C8a, C6–CO, and C8–CN bonds in both compounds. The side-chain carbonyl and amino groups were found to be coplanar with the pyrazole ring, in accordance with the experimental data (Fig. 4); however, notable discrepancies were observed for torsion angles of the triazine ring in **5** (e.g., C2–N1–C8a–N5, θ = 2.7(2)° and 13.8° for the experimental and DFT optimized structures, respectively).

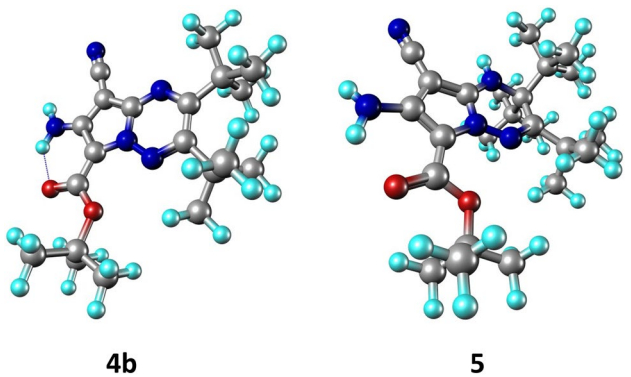

Fig. 5 Calculated (DFT B3LYP/6-31G(d), gas phase) structures of compounds **4b** and **5**

Hirshfeld surface analysis

Hirshfeld surface analysis (HSA) has proved to be a useful tool for enhancing exploration of the intermolecular interactions in crystals of a wide range of organic molecules [27] including heterocycles [36, 37]. To visualize the intermolecular contacts in the studied structures, HSA was performed as an additional method to X-ray diffraction analysis. In compounds 2a, 2e (hydrogen-bonded dimer),

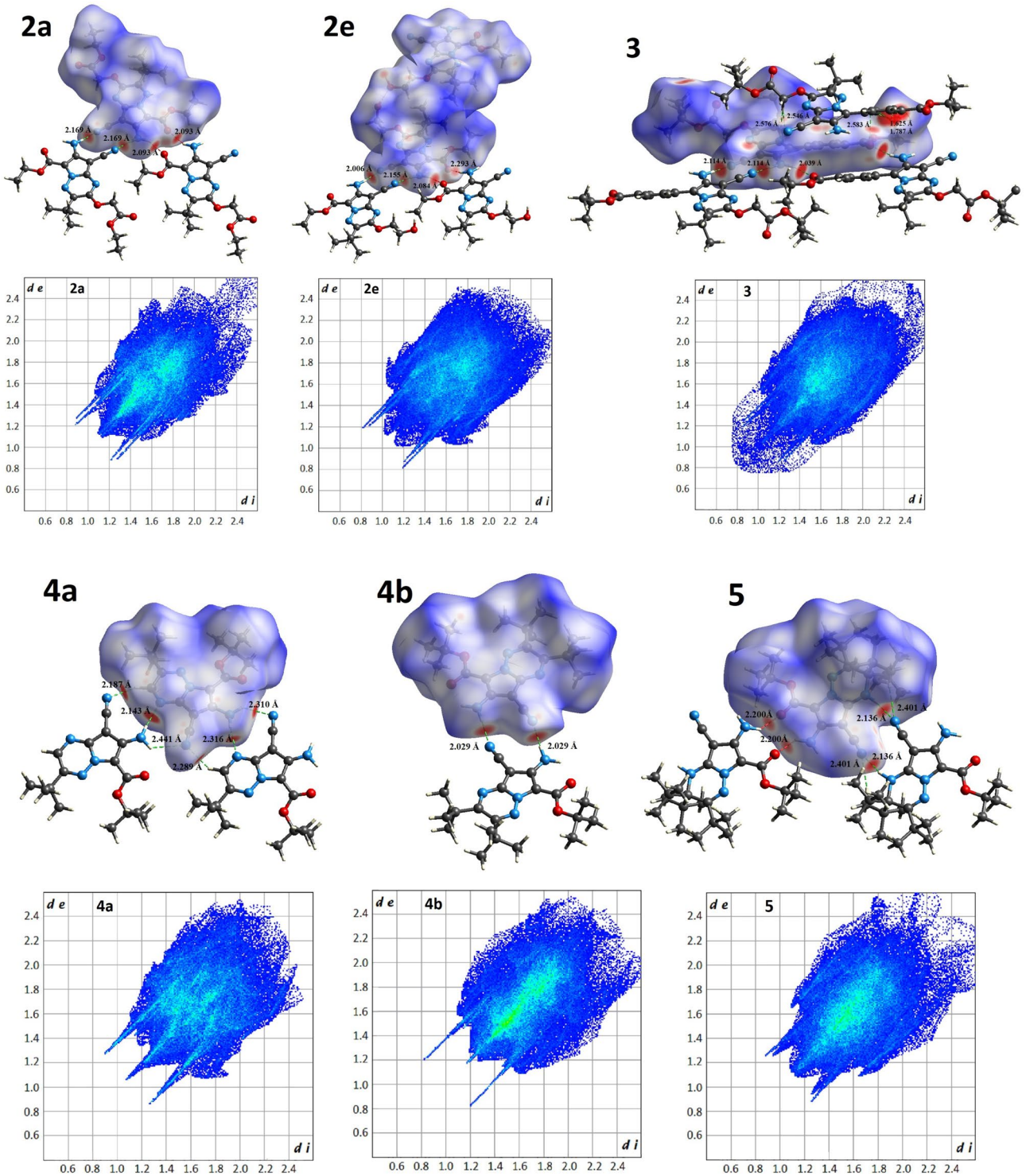

Fig. 6 The d_{norm} surfaces for 2a, 2e (hydrogen-bonded dimer), 3, 4a, 4b, and 5, H···N and H···O contacts (top) and their overall 2D fingerprint plots (bottom). Blue and red regions are weak and strong interactions, respectively. Isovalues range from − 0.39 to + 1.75 (**2a**), from − 0.48 to + 1.58 (**2e**), from − 0.25 to + 1.41 (**3**), from − 0.38 to + 1.60 (**4a**), from − 0.47 to + 1.62 (**4b**), and from − 0.38 to + 1.61 (**5**)

3, 4a, 4b, and 5, the main contribution to the energy of the non-valent interactions was made by the N···H bonds. For all the analyzed compounds, surface area also included the expected O···H reciprocal contacts (4.2% for 4b, 4.9% for 5, 6.1% for 4a, 11.1% for the dimer of 2e, 11.6% for 3, and 14.1% for 2a), which is consistent with the XRD data. These contacts are shown as colored sections on the graph of d_{norm} surfaces where $d_{norm} = d_i + d_e$ and red ($d_{norm} <$ VdW radii), blue ($d_{norm} >$ VdW radii), white ($d_{norm} =$ VdW radii) (Fig. 6). The intermolecular energies in crystal packing and the fingerprint plots with d_{norm} surfaces were calculated at B3LYP/6-31G(d) level of theory.

Analysis of the Hirshfeld surface for compound 3 also revealed notable H···H type of short contact between the isopropyl and phenyl groups which was not observed for other compounds. The calculated shortest interatomic distances $H_{i\text{-}Pr}\cdots H_{Ph}$ lied in range 1.625–1.787 Å and were in satisfactory agreement with the experimental X-ray diffraction analysis (1.6898–1.8790 Å). The reciprocal contacts between nearby molecules and the resulting fingerprint plots are shown on Fig. 6.

Conclusions

To summarize, a series of novel 7-amino-3-*tert*-butyl-8-cyanopyrrolo[1,2-*b*][1,2,4]triazine-6-(*p*-phenylene)carboxylates bearing different substituents in the C2 ring position (OCH_2CO_2Et, OCH_2Boc, OMe, OBu, OCH_2CH_2OH, H, *t*-Bu) have been synthesized by alkylation, 5-*exo*-dig cyclization, and nucleophilic substitution, and their structures were investigated by X-ray diffraction. The experimental results indicated the changes in the electron density distribution, as well as a marked increase in the bond lengths for the sterically hindered derivatives. The crystals of the studied compounds also showed diverse packing modes based on hydrogen bonding, which nature changed with the substitution pattern in heterocyclic nucleus and was successfully investigated by the DFT calculations and Hirshfeld surface analysis.

Supplementary Information The online version contains supplementary material available at https://doi.org/10.1007/s11224-022-02006-x.

Acknowledgements Crystal structure determination was performed in the Department of Structural Studies of Zelinsky Institute of Organic Chemistry, Moscow.

Author contribution The authors of the current manuscript Denis S. Koltun and Sergey M. Ivanov contributed equally to this work. All authors read and approved the final manuscript.

Data availability The structures have been deposited at the Cambridge Crystallographic Data Center with the reference CCDC numbers 2024439, 2024440, 2077346, 2077350–2077352, and 2,098,491; they also contain the supplementary crystallographic data. These data can be obtained free of charge from the CCDC via http://www.ccdc.cam.ac.uk/. The online version of this article contains electronic supplementary material (ESM) on crystal structures, IR, NMR, and HRMS data for all new compounds.

Code availability Not applicable.

Declarations

Conflict of interest The authors declare no competing interests.

References

1. Debnatha B, Singh WS, Das M, Goswami S, Singh MK, Maiti D, Manna K (2018) Role of plant alkaloids on human health: a review of biological activities. Mater Today Chem 9:56–72. https://doi.org/10.1016/j.mtchem.2018.05.001
2. Ain Q-U, Khan H, Mubarak MS, Pervaiz A (2016) Plant alkaloids as antiplatelet agent: drugs of the future in the light of recent developments. Front Pharmacol 7:292. https://doi.org/10.3389/fphar.2016.00292
3. Su C, Yan Y, Guo X, Luo J, Liu C, Zhang Z, Xiang W-S, Huang S-X (2019) Characterization of the *N*-methyltransferases involved in the biosynthesis of toxoflavin, fervenulin and reumycin from *Streptomyces hiroshimensis* ATCC53615. Org Biomol Chem 17:477–481. https://doi.org/10.1039/C8OB02847H
4. Ruanpanun P, Laatsch H, Tangchitsomkid N, Lumyong S (2011) Nematicidal activity of fervenulin isolated from a nematicidal actinomycete, *Streptomyces* sp. CMU-MH021, on *Meloidogyne incognita*. World J Microbiol Biotechnol 27:1373–1380. https://doi.org/10.1007/s11274-010-0588-z
5. Smirnov VV, Kiprianova EA, Garagulya AD, Esipov SE, Dovjenko SA (1997) Fluviols, bicyclic nitrogen-rich antibiotics produced by *Pseudomonas fluorescens*. FEMS Microbiol Lett 153:357–361. https://doi.org/10.1111/j.1574-6968.1997.tb12596.x
6. Ivanov SM (2022) 1,2,4-triazines and their benzo derivatives. Comprehensive heterocyclic chemistry IV (Fourth Edition) 9:29–180. https://doi.org/10.1016/B978-0-12-818655-8.00062-7
7. Voinkov EK, Drokin RA, Ulomsky EN, Chupakhin ON, Charushin VN, Rusinov VL (2020) Methods of synthesis for the azolo[1,2,4]triazines. Chem Heterocycl Compd 56:1254–1273. https://doi.org/10.1007/s10593-020-02808-z
8. Voinkov EK, Drokin RA, Fedotov VV, Butorin II, Savateev KV, Lyapustin DN, Gazizov DA, Gorbunov EB, Slepukhin PA, Gerasimova NA, Evstigneeva NP, Zilberberg NV, Kungurov NV, Ulomsky EN, Rusinov VL (2022) Azolo[5,1-*c*][1,2,4]triazines and azoloazapurines: synthesis, antimicrobial activity and *in silico* studies. ChemistrySelect 7(5):e202104253. https://doi.org/10.1002/slct.202104253
9. Ke Z, Lu T, Liu H, Yuan H, Ran T, Zhang Y, Yao S, Xiong X, Xu J, Xu A, Chen Y (2014) 3D-QSAR and molecular fragment replacement study on diaminopyrimidine and pyrrolotriazine ALK inhibitors. J Mol Struct 1067:127–137. https://doi.org/10.1016/j.molstruc.2014.03.036
10. Shi W, Qiang H, Huang D, Bi X, Huang W, Qian H (2018) Exploration of novel pyrrolo[2,1-*f*][1,2,4]triazine derivatives with improved anticancer efficacy as dual inhibitors of c-Met/VEGFR-2. Eur J Med Chem 158:814–831. https://doi.org/10.1016/j.ejmech.2018.09.050

11. Knapp RR, Tona V, Okada T, Sarpong R, Garg NK (2020) Cyanoamidine cyclization approach to remdesivir's nucleobase. Org Lett 22(21):8430–8435. https://doi.org/10.1021/acs.orglett.0c03052
12. Dao P, Lietha D, Etheve-Quelquejeu M, Garbay C, Chen H (2017) Synthesis of novel 1,2,4-triazine scaffold as FAK inhibitors with antitumor activity. Bioorg Med Chem Lett 27(8):1727–1730. https://doi.org/10.1016/j.bmcl.2017.02.072
13. Kumar A, Singh UK, Gupta P, Muzaffar F, Pathak P, Tomar PK (2016) Synthesis, molecular docking and evaluation of antiangiogenic activity and cellular metastasis potential of some triazine and pyrrolidin-2-one derivatives. Pharma Chem 8(10):259–273
14. Sherin DR, Geethu CK, Prabhakaran J, Mann JJ, Kumar JSD, Manojkumar TK (2019) Molecular docking, dynamics simulations and 3D-QSAR modeling of arylpiperazine derivatives of 3,5-dioxo-(2H,4H)-1,2,4-triazine as 5-HT1AR agonists. Comput Biol Chem 78:108–115. https://doi.org/10.1016/j.compbiolchem.2018.11.015
15. Ivanov SM, Tuzharov EI, Kolotyrkina NG (2021) Synthesis of 7-amino-3-*tert*-butyl-2-alkylthiopyrrolo[1,2-*b*]-[1,2,4]triazine-6-carboxylates. Russ J Org Chem 91(12):2453–2461. https://doi.org/10.1134/S1070363221120148
16. Ivanov SM (2020) Anionic cascade recyclization of pyrazolo[5,1-*c*][1,2,4]triazines to pyrrolo[1,2-*b*][1,2,4]triazine and [1,2,4]triazino[2′,3′:1,5]pyrrolo[3,2-*c*]isoquinoline systems. Tetrahedron Lett 61(42):152404. https://doi.org/10.1016/j.tetlet.2020.152404
17. Ivanov SM (2021) Reversed steric order of reactivity for *tert*-butyl and adamantyl-3-cyanomethylene-1,2,4-triazines. J Heterocycl Chem 58(6):1371–1378. https://doi.org/10.1002/jhet.4255
18. Ivanov SM, Shestopalov AM (2019) Metalated Azolo[1,2,4]triazines. I. Synthesis of 2-(6-*tert*-butyl-5-oxo-4,5-dihydro-1,2,4-triazin-3(2*H*)-ylidene)acetonitriles *via* ring opening degradation of 3-*tert*-butyl-7-lithio-4-oxo-4*H*-pyrazolo[5,1-*c*][1,2,4]triazin-1-ides. J Heterocycl Chem 56(8):2210–2220. https://doi.org/10.1002/jhet.3615
19. Ivanov SM (2021) Synthesis of 6-*tert*-butyl-3-dicyanomethylene-5-silagermyl- and digermyl-1,2,4-triazines. Phosphorus Sulfur Silicon Relat Elem 196(10):911–919. https://doi.org/10.1080/10426507.2021.1939347
20. Bruker (2018) APEX-III. Bruker AXS Inc., Madison, Wisconsin, USA
21. Krause L, Herbst-Irmer R, Sheldrick GM, Stalke D (2015) Comparison of silver and molybdenum microfocus X-ray sources for single-crystal structure determination. J Appl Cryst 48:3–10. https://doi.org/10.1107/S1600576714022985
22. Sheldrick GM (2015) SHELXT - integrated space-group and crystal-structure determination. Acta Cryst A71:3–8. https://doi.org/10.1107/S2053273314026370
23. Sheldrick GM (2015) Crystal structure refinement with SHELXL. Acta Cryst C71:3–8. https://doi.org/10.1107/S2053229614024218
24. Frisch MJ, Trucks GW, Schlegel HB, Scuseria GE, Robb MA, Cheeseman JR, Scalmani G, Barone V, Petersson GA, Nakatsuji H, Li X, Caricato M, Marenich A, Bloino J, Janesko BG, Gomperts R, Mennucci B, Hratchian HP, Ortiz JV, Izmaylov AF, Sonnenberg JL, Williams-Young D, Ding F, Lipparini F, Egidi F, Goings J, Peng B, Petrone A, Henderson T, Ranasinghe D, Zakrzewski VG, Gao J, Rega N, Zheng G, Liang W, Hada M, Ehara M, Toyota K, Fukuda R, Hasegawa J, Ishida M, Nakajima T, Honda Y, Kitao O, Nakai H, Vreven T, Throssell K, Montgomery JrJA, Peralta JE, Ogliaro F, Bearpark M, Heyd JJ, Brothers E, Kudin KN, Staroverov VN, Keith T, Kobayashi R, Normand J, Raghavachari K, Rendell A, Burant JC, Iyengar SS, Tomasi J, Cossi M, Millam JM, Klene M, Adamo C, Cammi R, Ochterski JW, Martin RL, Morokuma K, Farkas O, Foresman JB, Fox DJ (2016) Gaussian 09, Revision A.02, Gaussian, Inc., Wallingford CT
25. Spackman PR, Turner MJ, McKinnon JJ, Wolff SK, Grimwood DJ, Jayatilaka D, Spackman MA (2021) CrystalExplorer: a program for Hirshfeld surface analysis, visualization and quantitative analysis of molecular crystals. J Appl Cryst 54:1006–1011. https://doi.org/10.1107/S1600576721002910
26. Spackman MA, McKinnon JJ (2002) Fingerprinting intermolecular interactions in molecular crystals. Cryst Eng Comm 4(66):378–392. https://doi.org/10.1039/B203191B
27. Spackman MA, McKinnon JJ, Jayatilaka D (2008) Electrostatic potentials mapped on Hirshfeld surfaces provide direct insight into intermolecular interactions in crystals. Cryst Eng Comm 10(4):377–388. https://doi.org/10.1039/b715227b
28. Bordwell FG, Algrim D, Vanier NR (1977) Acidities of anilines and toluenes. J Org Chem 42(10):1817–1819. https://doi.org/10.1021/jo00430a039
29. Bodzioch A, Pomikło D, Celeda M, Pietrzak A, Kaszynski P (2019) 3-Substituted benzo[*e*][1,2,4]triazines: synthesis and electronic effects of the C(3) substituent. J Org Chem 84(10):6377–6394. https://doi.org/10.1021/acs.joc.9b00716
30. Qiu H, Rong J, Li S, Tong W, Zhang T, Yang L (2014) Preparation, crystal structure, thermal decomposition, and DFT calculation of a novel 3D infinite structure coordination polymer $[Na_2(H_2O)_4(ITDO)_2]_n$ (ITDO = 2*H*-imidazo-[4,5-e]-*as*-1,2,4-triazine-2,7-dihydro-3,6-dione). Z Anorg Allg Chem 641(2):424–429. https://doi.org/10.1002/zaac.201400413
31. Otera J (1993) Transesterification. Chem Rev 93(4):1449–1470. https://doi.org/10.1021/cr00020a004
32. Luisi R, Degennaro L, Colella M (2021) Lithium. Reference Module in Chemistry, Molecular Sciences and Chemical Engineering, Elsevier. https://doi.org/10.1016/B978-0-12-820206-7.00049-4
33. Gray M, Tinkl M, Snieckus V (1995) Lithium. Comprehensive. Organomet Chem II(11):1–92. https://doi.org/10.1016/B978-008046519-7.00092-7
34. Ishigaki Y, Shimajiri T, Takeda T, Katoono R, Suzuki T (2018) Longest C–C single bond among neutral hydrocarbons with a bond length beyond 1.8 Å. Chem 4(4):795–806. https://doi.org/10.1016/j.chempr.2018.01.011
35. Shoker T (2017) Synthesis of novel extremely sterically hindered tertiary alkylamines. Technische Universität Chemnitz, Dissertation, 1–208. https://nbn-resolving.org/urn:nbn:de:bsz:ch1-qucosa2-211092
36. Saeed A, Shabir G, Hökelek T, Flörke U, Mauricio FE (2021) Synthesis, conformation and Hirshfeld surface analysis of benzoxazole methyl ester as a versatile building block for heterocycles. Heliyon 7(9):e08042. https://doi.org/10.1016/j.heliyon.2021.e08042
37. Karaush-Karmazin N, Baryshnikov G, Minaev B (2022) Crystal structure and Hirshfeld surfaces analysis of Heterocyclic- and circulenes. MATEC Web of Conferences 355:01020. https://doi.org/10.1051/matecconf/202235501020